Magnetic resonance force microscopy of nuclear spins: Detection and manipulation of statistical polarization

H. J. Mamin, R. Budakian, B. W. Chui, and D. Rugar
IBM Research Division, Almaden Research Center, 650 Harry Road, San Jose, California 95120, USA
(Received 7 January 2005; published 5 July 2005)

We have detected and manipulated the naturally occurring $\sqrt{N}$ statistical polarization in nuclear spin ensembles using magnetic resonance force microscopy. Using protocols previously developed for detecting single electron spins, we have measured signals from ensembles of nuclear spins in a volume of roughly $(150\ \mathrm{nm})^3$ with a sensitivity of roughly 2000 net spins in a 2.5 h averaging window. Three systems have been studied, ^{19}F nuclei in CaF_2, and ^1H nuclei (protons) in both polymethylmethacrylate and collagen, a naturally occurring protein. By detecting the statistical polarization, we not only can work with relatively small ensembles, but we eliminate any need to wait a longitudinal relaxation time T_1 to polarize the spins. We have also made use of the fact that the statistical polarization, which can be considered a form of spin noise, has a finite correlation time. A method similar to one previously proposed by Carlson *et al.* [Bull. Am. Phys. Soc. **44**, 541 (1999)] has been used to suppress the effect of the statistical uncertainty and extract meaningful information from time-averaged measurements. By implementing this method, we have successfully made nutation and transverse spin relaxation time measurements in CaF_2 at low temperatures.

DOI: 10.1103/PhysRevB.72.024413 PACS number(s): 76.60.−k, 05.40.−a, 07.55.−w

I. INTRODUCTION

Magnetic resonance force microscopy (MRFM) combines ultrasensitive force detection with the principles of magnetic resonance to probe small volumes of electron and nuclear spins.[1–6] If the goal of single nuclear spin sensitivity can be reached, the technique may ultimately allow for three-dimensional molecular imaging with atomic resolution.[2] It might also function as a readout scheme for quantum computation.[7,8] While the technique is still far from achieving these challenging goals, steady progress has been made, as evidenced by the recent demonstration of detection of a single electron spin with a spatial resolution of 25 nm.[9]

The measurement protocols previously developed for small ensembles of electron spins did not require a mean spin polarization, but rather took advantage of the naturally occurring statistical polarization. For an ensemble of N spins, this polarization is of order $\sqrt{N}$, and can actually exceed the thermal (Boltzmann) polarization for small N. One of the purposes of the current work is to demonstrate that these protocols are applicable to detecting the statistical polarization of nuclear spins as well as electron spins. This approach is particularly valuable for nuclear spins, since the time required to polarize a nuclear spin ensemble can be exceedingly long at low temperatures. In this work, we verify the technique by studying ensembles of order $N=10^8$ nuclear spins in a volume of roughly $(150\ \mathrm{nm})$,[3] where we detect and manipulate the statistical polarization of order $\sqrt{N}=10^4$ net spins.

A second purpose of this work is to demonstrate a scheme to extract meaningful information in the presence of the spin noise[10–13] associated with the statistical polarization. It has recently been proposed that manipulation of such fluctuating statistical ensembles should be possible by making use of the finite correlation time of the fluctuations.[14,15] We have implemented a version of this scheme using MRFM, and have performed spin manipulations on statistical ensembles of ^{19}F and ^1H nuclei. Despite the fact that the magnitude and even the sign of the polarization fluctuates over time, this approach has allowed us to perform nutations and transverse spin relaxation measurements.

II. EXPERIMENTAL DETAILS AND PROTOCOLS

Two species of nuclear spins were studied in three different samples. First, we studied ^{19}F in a polished single crystal of CaF_2 (99.99% pure).[16] We also studied protons in two different systems, the polymer polymethylmethacrylate (PMMA), and the triple-helix protein collagen. PMMA has previously been studied with MRFM using the Boltzmann polarization.[17] The collagen was chosen to demonstrate the applicability of MRFM to the study of biomolecules. The PMMA sample was a 200 nm thick film that was spun onto a silicon wafer and baked at 175 °C. It was then metal coated with 75 Å Cr/200 Å Au to reduce charging effects. The collagen sample was prepared from a commercially available solution of rat-tail collagen in acetic acid (Type 1, BD Biosciences). A small drop of the solution was placed onto a silica substrate and allowed to air dry. The sample was further dried in vacuum at room temperature for 4 days before use, but otherwise no special preparations were made. All three systems have expected spin densities in the range of $4-6\times10^{22}\ \mathrm{spins/cm^3}$.

As shown in Fig. 1 and described in Ref. 12, our MRFM technique uses a magnetic tip mounted on the end of a vertically oriented ultrasensitive cantilever. The tip generates a strong magnetic field gradient (~1 G/nm). A rf field B_1 at frequency ω_{rf} is used to excite magnetic resonance within a thin resonant slice where the condition $B_0(x,y,z)=\omega_{rf}/\gamma$ is met. Here B_0 is due to the tip field plus an optional external field B_{ext}, and γ is the gyromagnetic ratio (4.2 kHz/G for

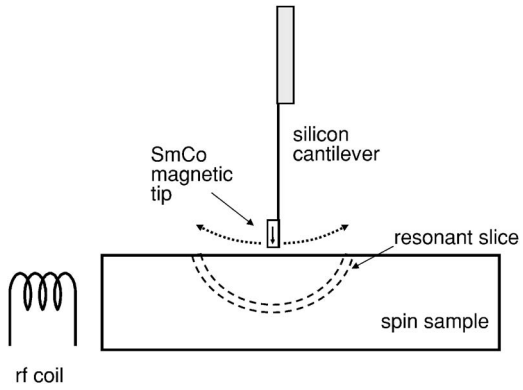

FIG. 1. Schematic of the MRFM experiment. Left-right statistical imbalance of the spin polarization within the resonant slice gives rise to forces on the magnetic tip.

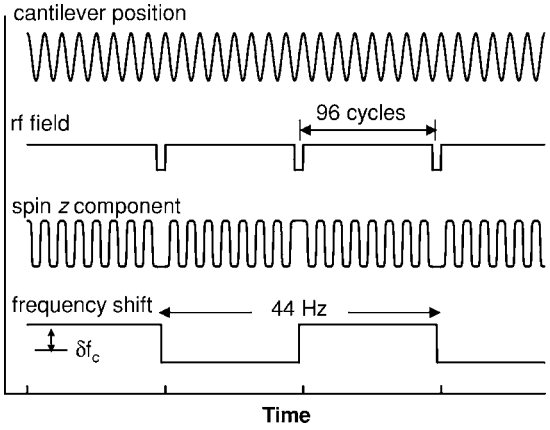

FIG. 2. Timing diagram for conventional iOSCAR protocol. As the cantilever oscillates, the z component of spin is modulated in response to the cantilever motion, except when the rf field is interrupted. These interruptions last for precisely one-half an oscillation period and occur every 96 cantilever cycles, leading to a modulation in the cantilever frequency.

protons and 4.0 kHz/G for ^{19}F). In the experiment on CaF_2, for example, the rf frequency was 50.8 MHz, so that the resonance condition was $B_0(x,y,z)=12\,680$ G. The rf field $B_1 \sim 15$ G was generated using a 300 μm diameter coil that was part of an *LC* resonant circuit. The microscope was operated in a small vacuum chamber within the bore of a superconducting magnet. The temperature of the microscope with the rf coil energized was roughly 7 K.

The same single-crystal silicon cantilever was used for all three samples. It consisted of a roughly 100 nm thick, 90 μm long shaft, with a 1 μm $\times$ 10 μm $\times$ 4 μm silicon mass on the end to suppress the motion of the higher order modes.[18] The cantilever spring constant k was roughly 8.6×10^{-5} N/m. In zero magnetic field, the cantilever resonant frequency f_c was 3830, and the quality factor Q was roughly 60 000 at 4.2 K. A SmCo particle was attached to the end of the cantilever with its magnetic axis carefully oriented in a magnetic field to within 5° of the cantilever axis, and then shaped with a focused ion beam to submicron dimensions to reduce its total moment. This preparation was necessary to prevent excessive cantilever bending in the applied magnetic field. The tip of the particle was further shaped to a roughly 250 nm wide apex, resulting in field gradients in the range of 1 G/nm. In a field of 12 000 G, the cantilever frequency increased to about 4200 Hz due to field-induced restoring torque, and the Q was reduced to approximately 5000 due to various magnetic loss mechanisms.[19,20] This undesirable effect, while not a major problem, can be eliminated through the use of an alternative cantilever orientation.[21]

The spin-manipulation and detection scheme is based on the OSCAR protocol used previously for electron spins,[9,12,22] where OSCAR stands for oscillating cantilever-driven adiabatic reversals. The cantilever is self-oscillated at its natural resonant frequency using a positive feedback loop. As the cantilever position oscillates according to $x_c(t)=x_{pk}\cos(\omega_c t)$, the field B_0 at a given sample location is modulated because of the field gradient $G=\partial B_0/\partial x$ from the tip. In the language of magnetic resonance, the effective field $\mathbf{B}_{eff}$ in the rotating frame is given by[12,23]

$$\mathbf{B}_{\mathrm{eff}} = B_1\hat{\mathbf{x}} + Gx_c(t)\hat{\mathbf{z}}. \tag{1}$$

For $Gx_{pk} \gg B_1$, $\mathbf{B}_{eff}$ will change from the $+\hat{z}$ to $-\hat{z}$ direction as the cantilever oscillates. As long as the adiabatic condition is met, the spins will be locked (or antilocked) to the effective field, and will thereby be synchronously inverted with each cantilever oscillation.[23] The backaction force of the spins on the cantilever gives rise to a slight cantilever frequency shift δf_c, whose sign depends on whether the spins are locked or antilocked to the effective field.

Rather than measure a dc frequency shift, we impose a modulation on the signal using an "interrupted" version of the protocol referred to as iOSCAR. As shown in Fig. 2, we turn off the rf power for one-half of a cantilever cycle every 96 cycles, which skips one adiabatic reversal, which, in turn, results in a change in the sign of the frequency shift δf_c. This imposes a modulation on the frequency shift at one-half the rf interrupt frequency, giving the signal a very distinctive signature. The frequency shift signal is analyzed using either a Fourier power spectrum or lock-in detector implemented in software. For statistical polarization, the mean lock-in signal is zero, so we detect the variance, or signal "energy." A zero-base line signal is constructed by subtracting the in-phase and quadrature variances. The optimal signal-to-noise ratio will be obtained when the lock-in time constant is properly matched to the spin-lock correlation time τ_m.[24] We use a bank of filters to obtain the signal as a function of measurement bandwidth, which is used to deduce τ_m.[9]

In the limit of $Gx_{pk} \gg B_1$, the cantilever frequency shift due to the spins is given by[25]

$$\delta f_c = (2f_c/\pi k x_{pk}) m_{\mathrm{eff}} G \tag{2a}$$

$$= (2f_c/\pi k x_{pk}) F_s, \tag{2b}$$

where m_{eff} is the component of magnetic moment along the effective field, and $F_s \equiv m_{eff}G$ represents the peak force exerted by the spins on the cantilever. Equation (2a) can be used to extract the effective number of spins contributing to the signal. Alternatively, Eq. (2b) can be used to convert the signal to a net force, which is useful when comparing signals at different cantilever amplitudes x_{pk}, for example.

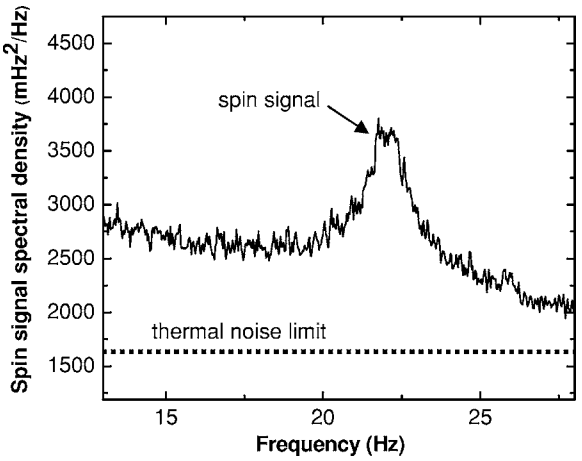

FIG. 3. Power spectral density of the frequency shift signal for the CaF_2 sample. An external field of 12 600 G was used to bring the sample into resonance, resulting in the statistical spin signal, seen as the peak at 22 Hz. The peak width of 1.9 Hz indicates a correlation time of roughly 170 ms. The estimated tip-sample separation was ~150 nm. The thermal noise limit for our cantilever with $Q=5000$ is indicated by the dotted line. The background noise level is higher than this level because of sample-induced excess frequency noise, which has a $1/f$-like spectrum.

III. MEASUREMENTS OF NUCLEAR STATISTICAL POLARIZATION

The power spectral density of the iOSCAR signal for the CaF_2 sample is shown in Fig. 3. The rf field was turned off every 96 cantilever cycles ($f_{\text{int}}=f_c/96\simeq 44$ Hz), resulting in a signal peak at 22 Hz. The spectral width of the peak is about 1.9 Hz, indicating a spin-lock correlation time τ_m of 0.17 s. This time is closely related to $T_{1\rho}$, the spin-lattice relaxation time in the rotating frame.[12,23] It can be affected by numerous parameters, such as the strength of the rf field, magnetic noise at the Rabi frequency due to higher order cantilever modes,[26,27] violation of the adiabatic condition, and the OSCAR protocol itself.[12,22] The latter two effects will be discussed later in the paper.

Scanning the external magnetic field B_{ext} moves the resonant slice relative to the tip, resulting in a signal when the slice penetrates into the sample. We plot the signal as a function of external field in Fig. 4(a), where the data represent the signal power from the lock-in detector in mHz^2. A zero base line signal is observed (within experimental error), with a large peak present in the range of ~12 000–13 000 G, where the width of the peak is inhomogeneously broadened due to the field gradient from the tip. Assuming an estimated field gradient of 1 G/nm, the maximum signal power of 1100 mHz^2 corresponds to $m_{eff}=1.7\times10^{-19}$ emu, or of order 10 000 net nuclear spins. The noise level obtained with an averaging time of 2.5 h was ~25 mHz^2, corresponding to roughly 2000 net nuclear spins. From Fig. 3, the integrated base line noise in the natural 1.9 Hz bandwidth was ~5000 mHz^2, corresponding to roughly 30 000 net spins.

Since we are not measuring the Boltzmann polarization, there is no need to wait a longitudinal relaxation time T_1 between measurements. For our CaF_2 sample, the measured

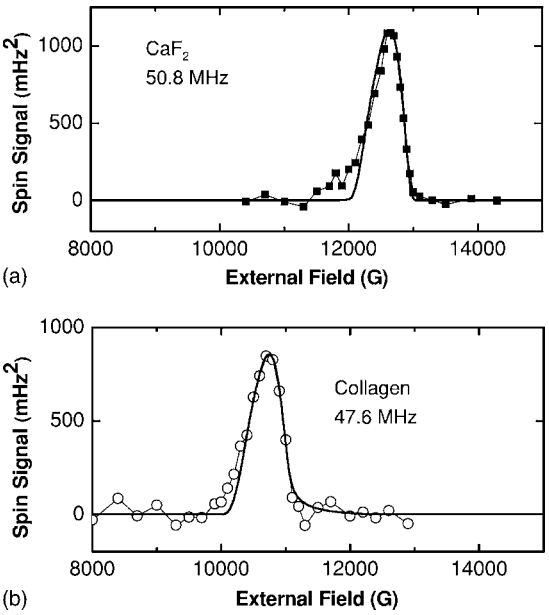

FIG. 4. MRFM signal vs externally applied magnetic field. (a) ^{19}F in CaF_2. The cantilever oscillation amplitude was 16 nm, and the applied rf frequency was 50.8 MHz, resulting in magnetic resonance when the total field is equal to 12 680 G. The continuous curve is calculated from a model based on a spherical tip with a diameter of 440 nm. In order to fit the model to the data, we had to assume a shift of +250 G in the field value at the location of the spins. This could be due to remanent magnetization in the body of our microscope, or a slight (2%) error in our field measurement. (b) Protons in collagen. The lower rf frequency, along with the higher gyromagnetic ratio for protons, result in a shift in the resonant field condition compared to ^{19}F.

T_1 was over 800 s at room temperature, and can be hours, days or longer in pure samples at low temperatures.[28,29] This consideration illustrates the significant advantage that can potentially be derived by working with the statistical polarization.

The MRFM signals from ^1H nuclei in PMMA and collagen were also readily detected. We plot the iOSCAR signal power as a function of B_{ext} for collagen in Fig. 4(b). The signal is seen in the range of $B_{ext}\sim 10\,000-11\,000$ G. As expected, the field range is lower than in the case of the CaF_2, partly because of the 5% higher gyromagnetic ratio in compared to ^{19}F, and partly because the rf frequency was slightly lower. In addition, the exact shape and position of the peak will depend on the distance between the tip and sample, which may have been somewhat less in the collagen sample.

The τ_m correlation times extracted from the lock-in detector data were disappointingly short, with $\tau_m\sim 200$ ms for CaF_2 and $\tau_m\sim 100$ ms for collagen. In the case of PMMA, the correlation times were less than 50 ms, and it was not possible to make an accurate measurement. In comparison, values of τ_m up to several seconds have been measured for E' centers (electron spins).[9,12] The shorter times observed here may be at least partly due to issues with these particular materials: CaF_2 requires a large field B_1 to overcome the local fields,[30] for example, while in PMMA, it is known that

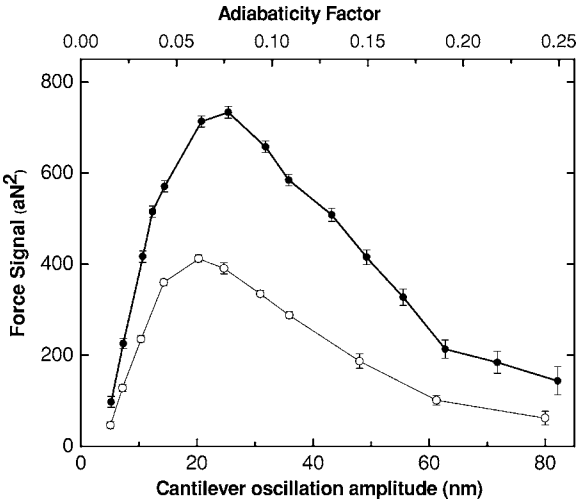

FIG. 5. Signal power vs cantilever oscillation amplitude for CaF_2. The open circles are for lower rf power ($B_1=15.5$ G) and the filled circles are for higher rf power ($B_1=18.1$ G). If the adiabatic reversals were equally effective under all conditions, the signal power would rise linearly from zero as a function of oscillation amplitude. In the case shown, the signal is diminished at the lowest amplitudes by the fact that the reversals are incomplete. At the higher amplitudes, the adiabatic condition is no longer met, which also reduces the signal.

tunneling of the methyl groups can occur over a wide frequency range and can affect the spin relaxation behavior.[31] At the same time, it is also likely that the iOSCAR protocol itself played a role.

For the iOSCAR protocol to work effectively, two conditions must be met. First, the field B_0 must be swept well off resonance; i.e., $Gx_{pk} \gg B_1$. As seen by Eq. (1), this ensures that the effective field, and thus the spins, are very nearly in the **z** direction when the cantilever reaches its extremum. Otherwise, each time the rf field is interrupted, the projected spin component along the effective field will be reduced. Second, the adiabatic condition $dB_0/dt \ll \gamma B_1^2$ must be satisfied.[23] A large value of x_{pk}, which drives the field B_0 farther off resonance, helps to satisfy the first condition. However, it hurts the second condition, since $dB_0/dt \propto x_{pk}$.

We observed that there was a fairly restricted range of cantilever oscillation amplitudes for which the iOSCAR protocol worked well. This is illustrated in Fig. 5, where the signal power vs oscillation amplitude x_{pk} is plotted for two different values of the rf field. For low oscillation amplitudes, the signal increased as x_{pk} was increased. This is partly because of the larger volume of spins being swept through by the resonant slice, but also because the field B_0 was being swept farther off resonance, leading to more complete adiabatic inversions. As x_{pk} was further increased, the signal reached a peak and then diminished, presumably due to violation of the adiabatic condition. We see that this decrease occurred for adiabaticity values, defined as $(dB_0/dt)/\gamma B_1^2$, greater than $\sim 8\%$. With a larger value of B_1 (upper curve), the signal was greater, and the optimum value for x_{pk} was somewhat larger as well.

The conflicting requirements of iOSCAR and the adiabatic condition can be eased in at least two ways. First, the condition $Gx_{pk} \gg B_1$ can be satisfied by reducing B_1 as the cantilever reaches its extremum. This type of rf pulse shaping was in fact performed in these measurements, and increased the signal by up to nearly a factor of 2. Second, decreasing the cantilever resonant frequency would allow for greater values of x_{pk} without violating the adiabatic limit. There may be lower practical limits on cantilever frequency, however, due to factors such as environmental vibrational noise.

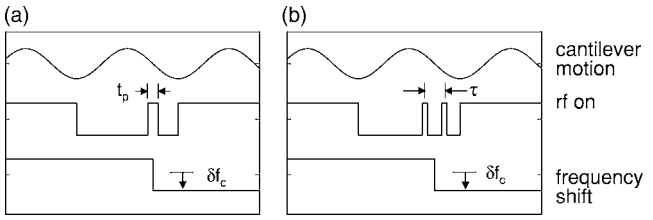

FIG. 6. Pulse sequences for use with modified iOSCAR that allow for manipulation of the statistical polarization. (a) Nutations. The rf field is interrupted for one full cantilever cycle every 96 cycles. Within the interruptions, the rf field is pulsed at the zero crossings. Those spins that are precisely on resonance will be begin to precess at the Rabi frequency about the effective field, which is in the x direction. Thus the z component will be a sinusoidal function of the pulse width T. (b) Transverse relaxation. Two $\pi/2$ pulses are inserted a time τ apart. For short τ, the effect is identical to a single π pulse. For long τ, the spins are left in a random direction in the x-z plane, and the spins are equally likely to be in the $+z$ and $-z$ directions when the field is turned back on.

IV. NUCLEAR SPIN MANIPULATION VIA MODIFIED iOSCAR

The above results verify that the protocols developed for detecting statistically polarized ensembles of electron spins are also applicable to nuclear spins. In addition to detection, the statistical polarization can also be manipulated into desired states through proper modification of the protocol. For example, we have previously demonstrated manipulation of the statistical polarization of electron spin ensembles using iOSCAR with extra rf interrupts in order to the rectify the spin fluctuations.[32]

In this section, we describe additional manipulation schemes that essentially compare the net polarization before and after a series of rf pulses. Because of its statistical nature, the initial state may be different each time the measurement is performed. Nevertheless, the pulses will affect the net polarization in some deterministic way that can be detected due to the finite correlation time of the polarization. The scheme is functionally very similar to a previously proposed scheme called CONQUEST (correlated observations narrow quantum uncertainty, enhancing spectroscopic transients), which is based on a second order correlation function of the signal before and after the pulse sequence.[14,15,33]

Our version of the detection protocol, illustrated in Fig. 6, is based on the iOSCAR protocol, with one key difference. The periodic interruptions in the rf field are now for one *full* cantilever cycle, rather than one half cycle. When the rf field is interrupted for one full cantilever cycle, a spin is left in

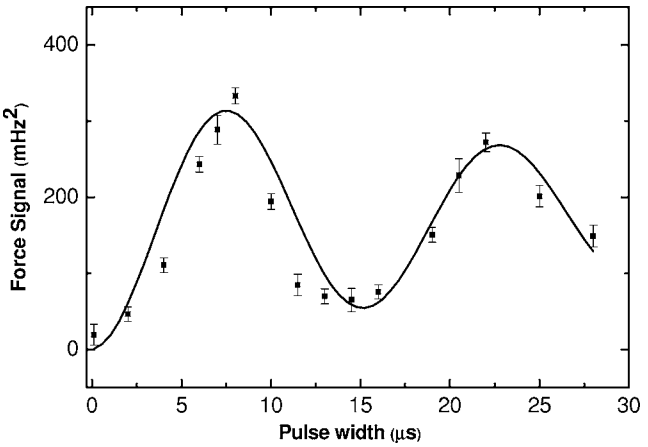

FIG. 7. Nutations of the statistical polarization in CaF_2. The modified iOSCAR signal is shown as a function of the pulse width t_p. The oscillatory nature of the signal is due to the precession of the spins about the effective field at the Rabi frequency. The period of the oscillations indicates a field strength $B_1=17$ G.

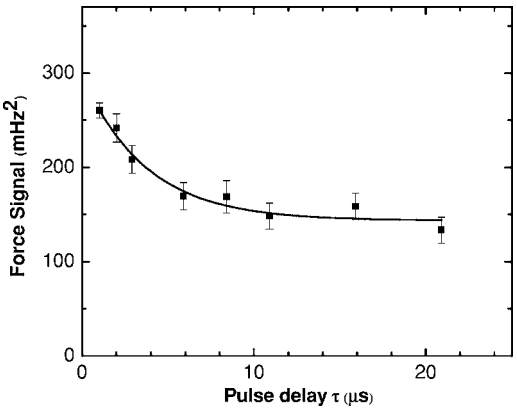

FIG. 8. Modified iOSCAR signal versus pulse delay τ. An exponential decay to the baseline is observed, indicating a transverse relaxation time $T_2^*=4$ μs.

exactly the same phase relative to the cantilever motion as when it started. Therefore no modulation of the frequency shift should occur. However, suppose that at every full-cycle rf interrupt, a rf pulse is inserted precisely on resonance, as shown in Fig. 6(a). The spins will nutate around the effective field, which in this case is in the **x** direction. If the pulse width t_p corresponds to a π pulse, the spins will end up inverted, and the situation will be equivalent to normal iOSCAR: A modulated frequency shift will be observed at half the interrupt frequency, which can be synchronously detected using a lockin amplifier. If the pulse width is 2π, then spins are left noninverted, and the modulation should again disappear. Thus the signal should show oscillatory behavior, with a period given by $2\pi/\gamma B_1$.

This protocol has allowed us to make our detection of nutations using a statistically polarized ensemble. The results for CaF_2 are shown in Fig. 7. For the case in which no nutation pulse is inserted during the rf interrupt ($t_p=0$), the signal is nearly zero, as expected. With a pulse inserted, the signal shows clear oscillatory behavior as a function of pulse width, with a period of roughly 15 μs. The measurement of the period allows for an absolute determination of the rf field strength, in this case $B_1=17$ G.

There is a close connection between this detection scheme and the CONQUEST scheme, as suggested by the following argument: Consider a model for the synchronous lock-in detection in which the basic signal $\delta f_c(t)$ is multiplied by a square wave of period $2T$ and then averaged. The resulting output signal then is made up of terms of the form $\delta f_c(t)-\delta f_c(t+T)$. (Here we have assumed that the square wave has no dc component. We also ignore correlations for times $\gtrsim T$, so that we can break up the time record into individual records of length $2T$, each of which is equivalent.) In this model, the mean square signal is simply the time average of $[\delta f_c(t)-\delta f_c(t+T)]^2$, or $2\langle \delta f_c(t)^2\rangle - 2\langle \delta f_c(t)\delta f_c(t+T)\rangle$, where $\langle\cdots\rangle$ denotes the time average. In normalized form, this is simply 1-A, where A is the same correlation function $\langle I_z(t)I_z(t+T)\rangle$ measured by CONQUEST in its most straightforward version.[33] In either case, the technique relies upon the systematic effect on the signal (such as inversion) caused by the inserted pulses. This results in a time-averaged correlation function $\langle \delta f_c(t)\delta f_c(t+T)\rangle$ that has a nonzero value, even if the initial values of $\delta f_c(t)$ are completely random. Note that since the modified iOSCAR scheme imposes a modulation on the signal, it has the added benefit of reducing the influence of low frequency noise.

A slightly different pulse sequence, illustrated in Fig. 6(b), has been used to measure the inhomogeneous transverse relaxation time T_2^*. Two $\pi/2$ pulses are inserted with variable spacing τ between them. The signal as a function of τ for CaF_2 is shown in Fig. 8. As expected, the signal is a maximum for small τ. This situation is equivalent to inserting a single π pulse, causing the spin polarization after the pulse sequence to be anticorrelated to the signal before the sequence. As seen with the nutation pulses, the result is a maximum in the iOSCAR signal. For large τ, the polarization after the pulse sequence is completely uncorrelated to that before, due to transverse relaxation, and one should get a signal that is one-half the maximum signal. (Alternatively, for small τ, the final polarization is the negative of the initial polarization, so the difference is twice the initial polarization. For large τ, the final polarization has decayed to zero, so the difference is half the difference in the short τ case.) This behavior is seen in Fig. 8, with a maximum signal for short τ, and an exponential decay to a base line that is roughly half the initial value. From the exponential decay, we find that that the transverse relaxation time $T_2^*=4$ μs. This short time is a reflection of the highly inhomogeneous field from the tip, which leads to a loss of phase coherence of the spins in physically different locations.

V. CONCLUSIONS

In summary, we have successfully applied the protocols developed for MRFM of electron spins to the case of nuclear spins. By performing iOSCAR to detect the statistical polarization in ensembles of nuclear spins, we have demonstrated

detection with sensitivity on the order of 2000 net nuclear spins in our 2.5 h averaging window. The statistical detection avoids the problem of the long T_1 times that exists for many nuclear spin systems at low temperatures. We have applied the technique to the system CaF_2, and have demonstrated our use of MRFM on a biomolecule. We have also demonstrated the ability to manipulate the naturally occurring statistical polarization in order to make nonequilibrium measurements, such as relaxation times and nutation measurements. Given a roughly 1000× improvement in signal-to-noise ratio, which remains a considerable challenge, these techniques should in principle be extendible to individual nuclear spins.

ACKNOWLEDGMENTS

We thank M. Sherwood, C. M. Jefferson, J. Logan, and C. Rettner for discussions and technical assistance. We gratefully acknowledge support from the DARPA Three-Dimensional Atomic-Scale Imaging program administered through the US Army Research Office.

[1] J. A. Sidles, Phys. Rev. Lett. **68**, 1124 (1992).
[2] J. A. Sidles, J. L. Garbini, K. J. Bruland, D. Rugar, O. Zueger, S. Hoen, and C. S. Yannoni, Rev. Mod. Phys. **67**, 249 (1995).
[3] D. Rugar, O. Zuger, S. Hoen, C. S. Yannoni, H. M. Vieth, and R. D. Kendrick, Science **264**, 1560 (1994).
[4] Z. Zhang, P. C. Hammel, and P. E. Wigen, Appl. Phys. Lett. **68**, 2005 (1996).
[5] K. R. Thurber, L. E. Harrell, R. Fainchtein, and D. D. Smith, Appl. Phys. Lett. **80**, 1794 (2002).
[6] S. R. Garner, S. Kuehn, J. M. Dawlaty, N. E. Jenkins, and J. A. Marohn, Appl. Phys. Lett. **84**, 5091 (2004).
[7] D. P. DiVincenzo, Phys. Rev. A **51**, 1015 (1995).
[8] G. P. Berman, G. D. Doolen, P. C. Hammel, and V. I. Tsifrinovich, Phys. Rev. B **61**, 14694 (2000).
[9] D. Rugar, R. Budakian, H. J. Mamin, and B. W. Chui, Nature (London) **430**, 329 (2004).
[10] F. Bloch, Phys. Rev. **70**, 460 (1946).
[11] T. Sleator, E. L. Hahn, C. Hilbert, and J. Clarke, Phys. Rev. Lett. **55**, 1742 (1985).
[12] H. J. Mamin, R. Budakian, B. W. Chui, and D. Rugar, Phys. Rev. Lett. **91**, 207604 (2003).
[13] S. A. Crooker, D. G. Rickel, A. V. Balatsky, and D. L. Smith, Nature (London) **431**, 49 (2004).
[14] P. L. Carlson, L. Madsen, G. M. Leskowitz, and D. Weitekamp, Bull. Am. Phys. Soc. **44**, 541 (1999).
[15] P. L. Carlson, L. A. Madsen, G. M. Leskowitz, and D. P. Weitekamp, U.S. Patent Nos. 6,078,082 and 6,081,119 (2000).
[16] Corning (formerly Optovac), North Brookfield MA.
[17] J. H. Choi, U. M. Mirsaidov, C. W. Miller, Y. J. Lee, S. Guchhait, M. D. Chabot, W. Lu, and J. T. Markert, Proc. SPIE **5389**, 399 (2004).
[18] B. W. Chui, Y. Hishinuma, R. Budakian, H. J. Mamin, T. W. Kenny, and D. Rugar, *Technical Digest of the 12th International Conference on Solid-State Sensors and Actuators (Transducers'03)*, (IEEE, Boston, MA, 2003), p. 1120.
[19] B. C. Stipe, H. J. Mamin, T. D. Stowe, T. W. Kenny, and D. Rugar, Phys. Rev. Lett. **86**, 2874 (2001).
[20] T. N. Ng., N. E. Jenkins, and J. A. Marohn (private communication).
[21] J. A. Marohn, R. Fainchtein, and D. D. Smith, Appl. Phys. Lett. **73**, 3778 (1998).
[22] B. C. Stipe, H. J. Mamin, C. S. Yannoni, T. D. Stowe, T. W. Kenny, and D. Rugar, Phys. Rev. Lett. **87**, 277602 (2001).
[23] C. P. Slichter, *Principles of Magnetic Resonance* (Springer, Heidelberg, 1996).
[24] M. Ting, A. O. Hero, D. Rugar, C.-Y. Yip, J. A. Fessler, preprint at http://xxx.lanl.gov/abs/quant-ph/0312139 (2003).
[25] G. P. Berman, D. I. Kamenev, and V. I. Tsifrinovich, Phys. Rev. A **66**, 023405 (2002).
[26] D. Mozyrsky, I. Martin, D. Pelekhov, and P. C. Hammel, Appl. Phys. Lett. **82**, 1278 (2003).
[27] G. P. Berman, V. N. Gorshkov, D. Rugar, and V. I. Tsifrinovich, Phys. Rev. B **68**, 094402 (2003).
[28] B. T. Beal and J. Hatton, Phys. Lett. **15**, 210 (1965).
[29] P. L. Kuhns, P. C. Hammel, O. Gonen, and J. S. Waugh, Phys. Rev. B **35**, 4591 (1987).
[30] K. Wago, O. Zuger, R. D. Kendrick, C. S. Yannoni, and D. Rugar, J. Vac. Sci. Technol. B **14**, 1197 (1996).
[31] A. J. Horsewill, Prog. Nucl. Magn. Reson. Spectrosc. **35**, 359 (1999).
[32] R. Budakian, H. J. Mamin, B. W. Chui, and D. Rugar (unpublished).
[33] L. A. Madsen, Ph.D. thesis, Caltech, 2002.